



Solid-ink-based print-and-peel method for microfluidic fabrication: a revisit

Sara Hopper¹ · Haipeng Zhang² · Sangjin Ryu^{2,3}

Received: 30 April 2019 / Revised: 15 July 2019 / Accepted: 25 July 2019 / Published online: 10 September 2019
© The Korean Society of Mechanical Engineers 2019

Abstract

The print-and-peel (PAP) method enables faster and cheaper fabrication of microfluidic devices, because this non-lithographic method uses a commercial printer to print channel mold patterns onto transparency film for use as a mold for microfluidic device fabrication. This study revisits the solid-ink-based PAP method by characterizing solid ink patterns printed on transparency films for cross-sectional shape, height, and surface roughness. In addition, the method was applied to create functional microfluidic devices to show that this low-cost method can be used for microfluidic applications.

Keywords Image processing · Microchannel · Non-lithographic microfluidic mold · Soft lithography · Surface topography · Wax printing

1 Introduction

Microfluidic devices have been widely employed because of their unique flow environments, but their use can be limited by fabrication difficulties with photo-lithography which requires specialized equipment in a clean-room environment. As an alternative non-lithographic approach, the print-and-peel (PAP) method was developed for easier and cheaper fabrication of microchannel devices [1]. This method involves generating channel patterns in a computer-aided design (CAD) program, making a mold by printing the channel pattern with a feature height of about 10 μm onto a transparency film, and curing polydimethylsiloxane (PDMS) over the mold. It is known that resulting mold surfaces have substantial roughness depending on the choice of printing technology.

Two types of office-grade printers have been used for the PAP method: laser printer [2–5] and solid-ink printer [6–8]. Although laser printers can produce microfluidic molds based on the PAP method, solid-ink printers have an advantage that their solid ink can be printed on nearly any media [9]. In addition, solid-ink printers print features with less roughness compared to laser printers [1]. In particular, this study focuses on the solid-ink-based PAP method.

Kaigala et al. proposed using a solid-ink printer for the PAP method [6]. They used a solid-ink printer for smooth features with a highest resolution setting of 2400 dpi, and tested regular Mylar film and specialized transparency film (Xerox Phaser solid-ink professional). They observed irregularity in printed solid-ink patterns due to occasional gaps in ink-coverage and rastering of the printing process. Thus, they proposed thermal treatment (warming the printed transparency for 10 min at 100 °C) to cause reflow of the solid ink and thus to further smoothen solid-ink reliefs. Kaigala et al. used a stylus profilometer to show that solid-ink features became smoother by the thermal treatment and had a maximum height of about 10 μm . They also recommended the specialized transparency film, because it had negligible number of speckles in contrast to Mylar film having random dark spots.

Despite promising results, however, Kaigala et al. [6] and following studies [7, 8] did not provide rigorous numerical data on the height and surface roughness of solid-ink-based microfluidic mold features, which is critical for other

Sara Hopper and Haipeng Zhang have contributed equally.

✉ Sangjin Ryu
sangjin.ryu@unl.edu

¹ Department of Bioengineering, Endicott College, Beverly, USA

² Department of Mechanical and Materials Engineering, University of Nebraska-Lincoln, Lincoln, USA

³ Nebraska Center for Materials and Nanoscience, Lincoln, USA

researchers to adopt the method. Therefore, this paper aims to further characterize the PAP method with solid-ink printing and to showcase applications of the method.

2 Materials and methods

2.1 Characterization of solid-ink patterns

Square patterns of $1.5\text{ mm} \times 1.5\text{ mm}$ were printed on transparency film in four different colors: cyan, yellow, magenta, and black with a solid-ink printer (Xerox ColorQube 8570) in the enhanced print-quality mode. Following Kaigala et al., two types of transparency film were used: Phaser solid-ink professional transparency film (Xerox) which is specialized for solid-ink printing, and Apollo laser printer transparency film (ACCO Brands) which is a generic brand. Kaigala et al. suggested heat treatment on solid-ink patterns for smoother surface [6], so we performed thermal treatment to some patterns by placing them on a hot plate at $80\text{ }^\circ\text{C}$ for 10 min.

The surface of the printed squares was imaged using a laser confocal scanning microscope (LCSM; Keyence VK-X200 K) at $10\times$ magnification. The lateral resolution and vertical resolution of the LCSM were $1.4\text{ }\mu\text{m}$ and 0.1 nm , respectively. This vertical resolution is comparable to that of a typical stylus profiler, while the lateral resolution is about one order of

magnitude lower than that of the stylus profiler. Although it was possible to achieve higher lateral resolution with the LCSM using a lens with higher magnification, $10\times$ magnification was chosen considering imaging time and solid-ink pattern size.

2.2 Image processing

The height and surface roughness of the solid-ink patterns were determined by image processing (Fig. 1). Obtained images were pre-processed using VK Analyzer (Keyence) for tilt correction and median-filter-based noise removal (Fig. 1a).

Then, images were imported as a .csv file into MATLAB (MathWorks), and converted and normalized in the gray scale to increase contrast between the pattern and background (Fig. 1b). A minimum bounding rectangle was fitted to the binary image of the imported image [10] to determine the center and angle of rotation of the pattern (Fig. 1c), and the imported image was rotated with respect to the center of the bounding box to be parallel to horizontal and vertical axes (Fig. 1d).

The height of the solid-ink pattern was determined as follows. The location of the film surface was determined by fitting a horizontal plane against the pixels outside the bounding box, and the film surface was found not to be at zero in the z -direction (Fig. 1e). Therefore, the image was adjusted, so that the z location of the film surface would

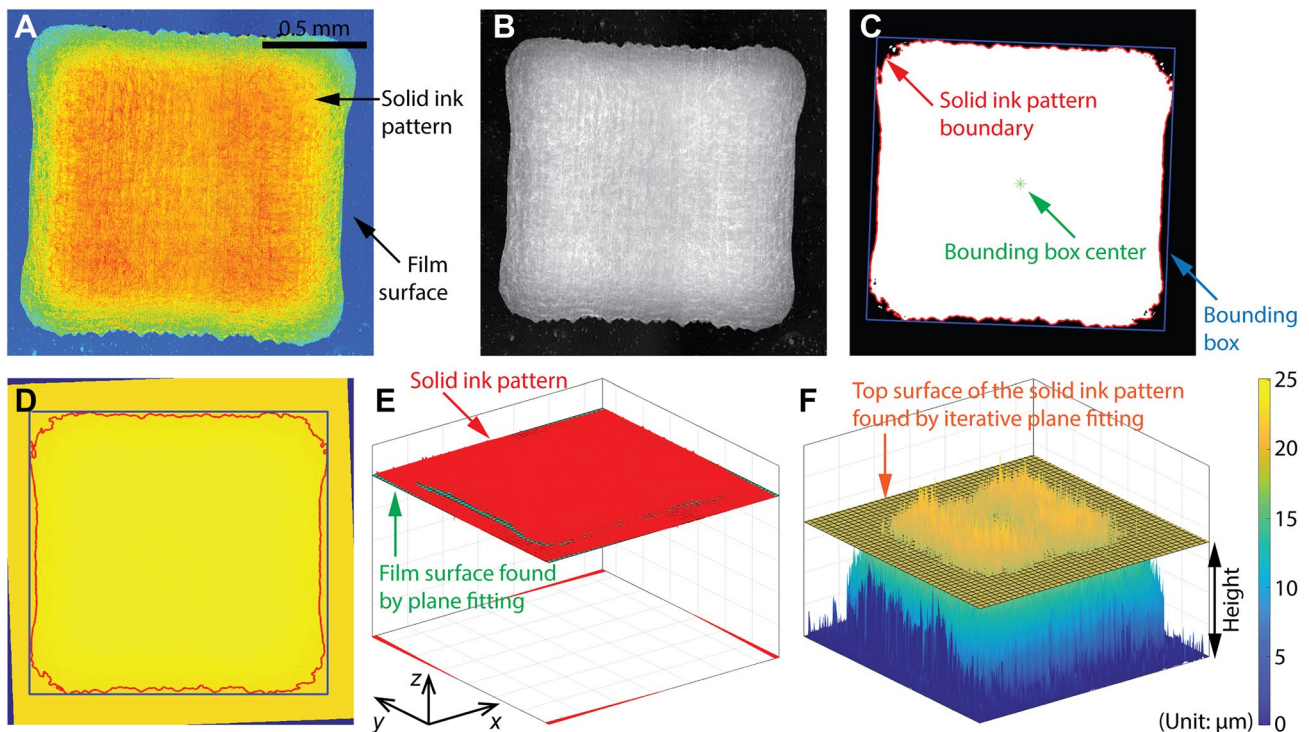


Fig. 1 MATLAB-based image processing to determine the height and surface roughness of solid-ink patterns. **a** Laser confocal scanning microscopy (LCSM) image of a solid-ink pattern. **b** Normalized

image in the gray scale. **c** Binary conversion, boundary detection, and bounding box determination. **d** Rotated image. **e** Film surface determination. **f** Top surface determination

be zero (Fig. 1f). Then, the top surface of the ink pattern was determined by iterative plane fitting (Fig. 1f). In this process, the plane fitting was done first against the pixels in the bounding box, and repeated for the pixels above the fitting plane until the vertical location of the fitting plane approached a certain value. Then, the height of the pattern (H) was determined, as shown in Fig. 1f.

Averaged cross-section of the pattern was determined by averaging cross-sections in either x - or y -directions across a half of the pattern (Fig. 2a top left panel; x - and y -directions are shown in Fig. 1e). Then, the region of interest for surface roughness estimation was determined by identifying the intersection points of the average cross-sections with the found top plane. Finally, the root-mean-square surface roughness (ϵ_{rms}) of the pattern was calculated from the region of interest.

2.3 Channel fabrication using soft lithography

Three microfluidic devices were fabricated using the PAP method: straight channel, Y channel, and serpentine channel. Channel designs were printed in black solid ink on the generic transparency film. A non-stick coating was applied using (tridecafluoro-1,1,2,2-tetrahydrooctyl)-1-trichlorosilane (T2492-KG, United Chemical Specialties). PDMS (Dow Corning Sylgard 184; 10:1 weight ratio of monomer and the curing agent) was poured on the mold, degassed, cured overnight at room temperature, and then cured at 55 °C for 1–2 h. PDMS curing at higher temperature resulted in adhesion of solid ink on PDMS.

The PDMS was peeled from the mold, and inlet and outlet holes were punched with a 0.5 mm biopsy punch. The

channel body was bonded to a slide glass using plasma activation. The device was connected to syringes using silicon tubing (Cole-Parmer), and dyed water was injected into the device using a syringe pump (Chemyx Fusion 200).

3 Results

3.1 Height and roughness of solid-ink patterns

LCSM imaging captured successfully the shape and surface roughness of the solid-ink patterns. Figure 2 shows black solid-ink patterns printed on the generic (Apollo) and specialized (Xerox) transparency film with and without heat treatment as examples. The optical images of as-is solid-ink patterns show raster lines from printing on the both transparency film types, as reported by the previous studies [6]. The LCSM images show that the raster lines were actually protruding (or convex, higher than the rest of the surface). Uneven wavy edges were present in the direction of the raster lines. Both transparency film types had visual imperfections on their surfaces, in contrast to the observation of Kaigala et al. [6], which might have affected the roughness of the printed pattern.

The developed MATLAB-based image processing successfully quantified the dimension and surface roughness of the sample patterns. The lateral dimension of the pattern was measured to be about 1.5 mm, similar to the intended size. Average cross-sectional images were obtained by averaging cross-sections of a pattern in the raster line direction and its normal direction (red and blue arrows in Fig. 2, respectively) using its LCSM image. The raster lines observed in

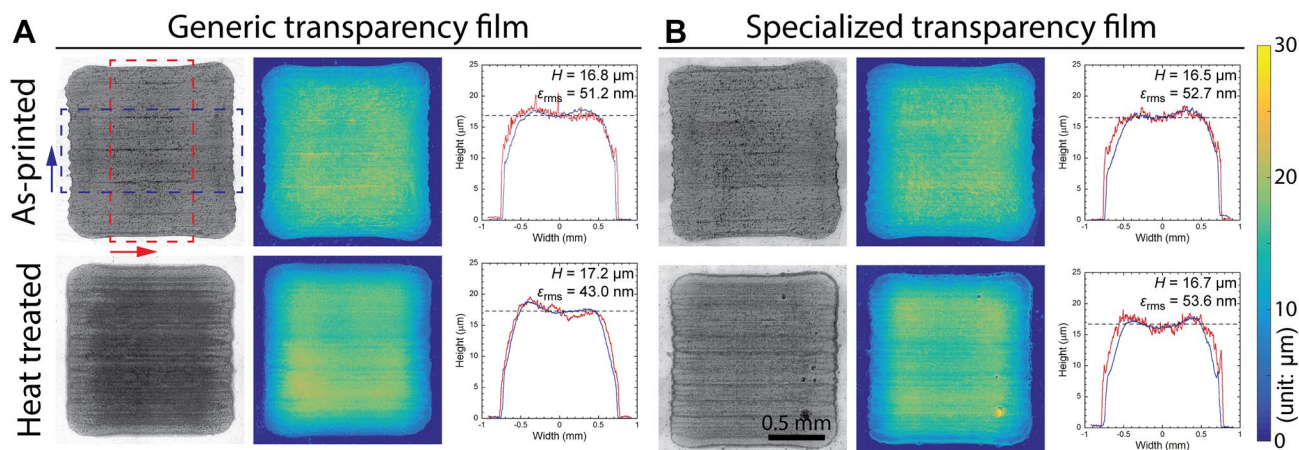


Fig. 2 Surface topography and height of square solid-ink patterns. **a** Generic film (Apollo laser printer transparency film). **b** Specialized film (Xerox Phaser solid-ink professional transparency film). Results of each case are shown in the order of optical image of the pattern, the surface topography image of the pattern (color bar shown on the right end of the figure), and the averaged cross-sectional image of

the pattern (the dashed boxes and arrows in the first image show the averaging direction and area for the cross-section plot; the horizontal dashed lines show the height of the solid-ink pattern determined in Fig. 1). H pattern height, ϵ_{rms} root-mean-square roughness of pattern surface

microscopy images can be seen in the cross-sectional image averaged in the raster line direction, whereas the other averaged cross-section shows less conspicuous roughness pattern. The both cross-sections are in approximate trapezoidal shapes, which are ideal for microfluidics, and they agree well with the top surface of the solid-ink pattern, which was found by the iterative plane fitting process done against the whole solid-ink pattern (dashed lines in the cross-section plots of Fig. 2).

Some of the prepared samples were heat treated following the method of Kaigala et al. [6]. The thermal treatment was found to have smoothed the surface of the solid-ink patterns somewhat (Fig. 2). However, the height and surface roughness of the heat-treated samples were not different from those of non-treated ones. In addition, the thermal treatment sometimes resulted in undesirable effects on solid-ink patterns such as unevenness in height or surface roughness. Therefore, we exclude heat-treated samples in the following analysis and device fabrication.

To determine the range of the height and surface roughness of solid-ink molds for microfluidics, 4 or 5 solid-ink square patterns of four different colors were imaged using LSCM. The height and surface roughness range of the solid-ink patterns were about 17 μm and 45–55 nm, respectively (Table 1). Our height measurement agrees well with the previous studies (Kaigala et al. [6]: $\sim 10 \mu\text{m}$, Thomas et al. [1, 8]: 10–15 μm). There were no significant differences between color of solid-ink patterns in terms of height or roughness.

3.2 Minimum channel width

In terms of practical applications of the PAP method, it is important to know the minimum channel width achievable with the method. Straight microchannels with different channel widths were fabricated and tested by injecting red-dyed water through the channels (Fig. 3a). It was found that water could flow through even the 0.1 mm-wide channel.

To confirm our observation, we measured the width of straight lines printed in solid ink (Fig. 3b). The actual width of 0.01, 0.05, 0.1, 0.2, 0.3, and 0.5 mm-wide lines was

Table 1 Height and roughness of printed solid-ink patterns (mean \pm std)

	Generic film		Specialized film	
	Height (μm)	Roughness (nm)	Height (μm)	Roughness (nm)
Black	16.6 \pm 0.2	54.6 \pm 3.3	16.6 \pm 0.2	44.7 \pm 6.3
Cyan	17.9 \pm 0.3	50.4 \pm 8.8	17.8 \pm 0.2	45.2 \pm 5.9
Magenta	17.6 \pm 0.1	52.0 \pm 8.0	17.8 \pm 0.1	52.0 \pm 19.0
Yellow	16.9 \pm 0.6	47.5 \pm 5.4	16.8 \pm 0.4	50.6 \pm 7.5

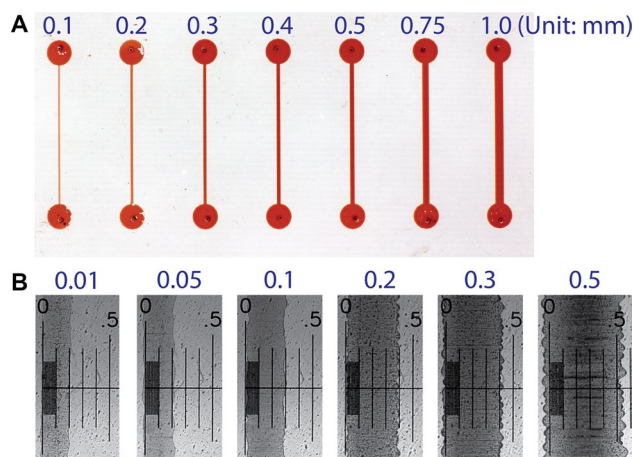


Fig. 3 Minimum width of channels fabricated with the solid-ink-based print-and-peel method. **a** Straight channel test to determine the minimum channel width for fluid flow. **b** Measurement of the width of solid-ink lines using a calibration slide (one grid=0.1 mm). Numbers shown in blue are the design values for the channel width (unit: mm)

measured to be around 0.2, 0.2, 0.3, 0.4, 0.4, and 0.5 mm, respectively. This result shows that the actual width of printed channels was larger than the design value when they were designed to be narrower than 0.5 mm, and the achievable minimum channel with the employed PAP method is about 200 μm . Our result agrees well with the results of Thomas et al. [1, 8]. They measured the channels made of the solid-ink-based PAP method to be 250 μm [8]. In addition, they showed that the minimum line width of solid-ink patterns was about 300 μm [1]. Kaigala et al. also pointed out that the smallest widths achievable with office-grade solid-ink printers were $\sim 300 \mu\text{m}$ [6].

3.3 Examples of fabricated devices

Microfluidic devices were successfully fabricated with the PAP method. Red and green dyes were able to be perfused through the two inlets of the Y channel (Fig. 4a), and mixing between the two colors was very limited in the main channel as seen by the clear separation between the colors. To test the observed limited mixing, we fabricated a very long serpentine channel (Fig. 4b). Although the channel length was much longer than the Y channel, the two colors were still separated till the outlet. We also fabricated Christmas tree microchannel devices which are widely used for generating concentration gradient, but no clear concentration gradient was created due to limited mixing.

The inset of Fig. 4a shows that the surface roughness pattern of the solid-ink mold was also seen in the surface of the fabricated channel. We compared LCSM images of a solid-ink mold and a PDMS replica of the mold to check how well soft lithography could replicate the mold in the

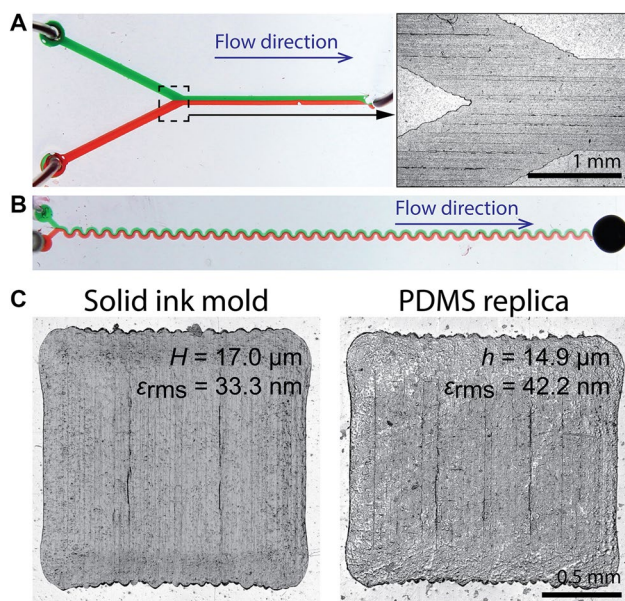


Fig. 4 Microfluidic channels fabricated with the solid-ink-based print-and-peel method. **a** Y channel showing limited mixing between two colors. Inset: microscopic image of the PDMS channel surface showing surface roughness and raster lines imprinted by solid-ink mold. **b** About 100 mm-long serpentine channel showing limited mixing. **c** Comparison of a solid-ink mold and its PDMS replica. h the channel height

solid-ink-based PAP method. As shown in Fig. 4c, the PDMS replica overall maintained the key features of the solid-ink mold except smudged features along the perimeter. The height of the PDMS replica was about 6% lower than that of the mold, whereas the surface roughness increased by 27%.

However, it is expected that this level of roughness of the channel surface cannot affect the flow significantly for two reasons. First, the relative surface roughness was about $\varepsilon_{\text{rms}}/h \approx 0.003$, which has negligible effects even for high Reynolds number flows. Here, h is the channel height. Second, laminar flows are not disturbed by surface roughness [5]. As shown in Fig. 4a and b, laminar flow in the long channel was not disturbed by the rough surface.

The observed limited mixing can be understood by estimating the flow distance of the fluids through the channel required for complete mixing. The width (w) of the serpentine channel was 0.5 mm. The inject volume flow rate (Q) was 0.05 ml/min, and thus, the average flow speed (V) was 0.11 m/s with the approximate channel height of 15 μm . The mixing time across the channel can be estimated using $t_{\text{mix}} \sim w^2/D$, where D is the diffusion coefficient [11]. With a typical D value for ions ($2 \times 10^{-9} \text{ m}^2/\text{s}$) [11], t_{mix} was found to be ~ 125 s. During t_{mix} , the fluid would have flowed over ~ 14 m ($= Vt_{\text{mix}}$) which is two orders of magnitude longer than the channel length (≈ 0.1 m). Therefore, complete mixing cannot be achieved in this channel even with

the high D value. In this case, the Péclet number ($Pe = Vw/D$ [11]) was about 2.75×10^4 .

4 Discussion

The PAP method is an alternative microfluidic mold fabrication method for photo-lithography, which can decrease the total fabrication cost and time of microfluidic devices. When the method was proposed, laser printers were used to print out CAD-designed mold on a transparency film [2–5]. Channel reliefs made of toner particles were found to have a trapezoidal cross-section with a height of 6–14 μm and a surface roughness of 0.2–1.2 μm .

Solid-ink printers were also employed for the PAP method, and solid-ink-relief of printed molds was found to be smoother than those printed by laser printers [8]. Another advantage of solid-ink printing is that solid ink can be printed on virtually all types of media, including paper and plastic film [9].

Solid ink is commonly made from a combination of paraffin wax, resin, and dye [12], and it has a typical melting temperature of around 90 $^{\circ}\text{C}$ [9, 12, 13]. Kaigala et al. proposed warming solid-ink molds for 10 min at 100 $^{\circ}\text{C}$ to decrease the roughness of solid-ink reliefs, and they pointed out that a specific condition for the thermal treatment needs to be determined empirically [6]. We tried the proposed thermal treatment method and found that 100 $^{\circ}\text{C}$ was too high. After thermal treatment at 100 $^{\circ}\text{C}$, solid-ink reliefs showed significant changes in their shape due to significant reflow of molten solid ink. For instance, the solid-ink patterns were in the trapezoidal pyramid shape, as shown in Fig. 2, but their shape changed to the mound shape after the 100 $^{\circ}\text{C}$ thermal treatment. Li et al. measured that the viscosity of solid inks significantly decreased around 90 $^{\circ}\text{C}$ [13]. Therefore, we decreased the temperature for the thermal treatment to 80 $^{\circ}\text{C}$ and could avoid the reflow problem. However, no significant differences in feature height and surface roughness were found between as-printed patterns and thermally treated patterns (Fig. 2).

The aforementioned relatively low melting point of the solid-ink limits curing of PDMS over the solid-ink-printed masters at elevated temperature [1]. We found that molten solid ink was left on cured PDMS when PDMS was cured at 80 $^{\circ}\text{C}$ on solid-ink-printed channel molds. Therefore, we cured PDMS at room temperature overnight and then at 55 $^{\circ}\text{C}$ for 1–2 h.

Kaigala et al. recommended using Xerox Phaser solid-ink professional transparency film, specialized for solid-ink printers, because generic Mylar film showed random dark spots [6]. According to the manufacturer of the used solid-ink printer [14], the Phaser transparency film is more receptive to solid-ink features, whereas generic transparency

films leave raised edges of ink features. Accordingly, we compared the specialized film and the generic transparency film (Apollo). Our imaging and analysis showed negligible difference between the two film types (Table 1 and Fig. 2). Therefore, we think that the generic transparency film can be used for the medium to print solid-ink channel patterns.

The solid-ink-based PAP method was successfully used for fabricating a few simple microfluidic channels. We found that the minimum channel width achievable with the method was about 200 μm (Fig. 3b) and that the actual channel height was about 15 μm (Fig. 4c). Based on these results, the minimum aspect ratio of the microchannel achievable using the solid-ink-based PAP method was estimated to be about 13. According to Thomas et al. [1], solid-ink printers could not print out features with lateral dimensions smaller than $\sim 200 \mu\text{m}$. Our experiments using the Y channel and the serpentine channel showed that injected red and green dyed water were clearly separated all through the channels because of very small channel height (Fig. 4a, b). Similarly, Thomas et al. did not observe even partial mixing in the PAP-fabricated microchannels at a relatively high volume flow rate of 0.4 ml/min [8].

5 Conclusion

The solid-ink-based PAP method is an effective non-lithographic method for easier and cheaper fabrication of microfluidics master mold. To provide potential users of this method with reference data, we characterized solid-ink-based master molds printed on transparency film using laser confocal scanning microscopy and automated image processing. The typical height and surface roughness of printed solid-ink molds were $\sim 17 \mu\text{m}$ and $\sim 50 \text{ nm}$, respectively. Heat treatment on printed solid-ink patterns did not improve mold surface significantly, and the type of used transparency types did not affect mold surface quality significantly. We could apply the solid-ink-based PAP method successfully for real microfluidic device fabrication.

Although this method's low cost and ease-of-use lead to it being an inexpensive, promising alternative to other common fabrication methods, the method has major limitations: the thickness of fabricated molds is fixed at $\sim 17 \mu\text{m}$ with surface roughness of $\sim 50 \text{ nm}$, and the channel width cannot be smaller than 200 μm . These limitations result in relatively high aspect ratio of fabricated channels, and very limited mixing in channels. Therefore, the solid-ink-based PAP method needs to be employed with these limitations considered.

Acknowledgements This study was supported by an Interdisciplinary Research Grant from the University of Nebraska-Lincoln, USA and by the National Science Foundation Research Experiences for Undergraduates (grant #1659777). Microscopy imaging was performed at the NanoEngineering Research Core Facility (part of the Nebraska Nanoscale Facility), which is partially funded from the Nebraska Research Initiative.

Compliance with ethical standards

Conflict of interest On behalf of all authors, the corresponding author states that there is no conflict of interest.

References

1. M.S. Thomas, B. Millare, J.M. Clift, D. Bao, C. Hong, V.I. Vullev, Print-and-peel fabrication for microfluidics: What's in it for biomedical applications? *Ann. Biomed. Eng.* **38**, 21–32 (2010)
2. A. Tan, K. Rodgers, J.P. Murrhiy, C. O'Mathuna, J.D. Glennon, Rapid fabrication of microfluidic devices in poly(dimethylsiloxane) by photocopying. *Lab Chip* **1**, 7–9 (2001)
3. M.L. Branham, R. Tran-Son-Tay, C. Schoonover, P.S. Davis, S.D. Allen, Rapid prototyping of micropatterned substrates using conventional laser printers. *J. Mater. Res.* **17**, 1559–1562 (2002)
4. N. Bao, Q. Zhang, J.-J. Xu, H.-Y. Chen, Fabrication of poly(dimethylsiloxane) microfluidic system based on masters directly printed with an office laser printer. *J. Chromatogr. A* **1089**, 270–275 (2005)
5. V.I. Vullev, J. Wan, V. Heinrich, P. Landsman, P.E. Bower, B. Xia, B. Millare, G. Jones, Nonlithographic fabrication of microfluidic devices. *J. Am. Chem. Soc.* **128**, 16062–16072 (2006)
6. G.V. Kaigala, S. Ho, R. Peterman, C.J. Bachouse, Rapid prototyping of microfluidic devices with a wax printer. *Lab Chip* **7**, 384–387 (2007)
7. C. Hong, D. Bao, M.S. Thomas, J.M. Clift, V.I. Vullev, Print-and-peel fabrication of microelectrodes. *Langmuir* **24**, 8439–8442 (2008)
8. M.S. Thomas, J.M. Clift, B. Millare, V.I. Vullev, Print-and-peel fabricated passive micromixers. *Langmuir* **26**, 2951–2957 (2010)
9. R.L. Adams, Phase change ink jet technology. In: Rezanka I, Eschbach R (eds) *Recent progress in ink jet technologies*. The Society for Imaging Science and Technology (1996), pp. 138–141
10. J. Diener, 2D minimal bounding box version 1.1.0.0, MATLAB Central File Exchange (2011). <https://www.mathworks.com/matlabcentral/fileexchange/31126-2d-minimal-bounding-box>
11. T.M. Squires, S.R. Quake, Microfluidics: Fluid physics at the nanoliter scale. *Rev. Mod. Phys.* **77**, 977–1026 (2019)
12. A. Pekarovicova, H. Bhide, P.D. Fleming III, J. Pekarovic, Phase-change inks. *J. Coat. Technol.* **75**, 65–72 (2003)
13. R. Li, N. Ashgriz, S. Chandra, J.R. Andrews, Shape and surface texture of molten droplets deposited on cold surfaces. *Surf. Coat. Technol.* **202**, 3960–3966 (2008)
14. Xerox Phaser Solid-Ink Transparencies, SUPFS-02UC-02. <https://www.office.xerox.com/latest/SUPFS-02.PDF>



Sara Hopper is currently pursuing her Ph.D. degree in biomedical engineering at the University of Michigan, Ann Arbor, MI, USA. She received her B.S. degree in bioengineering from Endicott College, Beverly, MA, USA.



Haipeng Zhang is currently a Ph.D. student of the Department of Mechanical and Materials Engineering, University of Nebraska-Lincoln (UNL), Lincoln, Nebraska, USA. He received the B.S. degree in Mechanical Engineering from Kitami Institute of Technology, Kitami, Japan, in 2007, and the M.S. degree in Mechanical Engineering and Applied Mechanics from UNL in 2018. He also worked for Kubota Corporation (Japan) in Beijing, China, during 2009–2015. He was the recipient

of Graduate Student Scholarship Award from the ASME Fluids Engineering Division for ASME–JSEM–KSME Joint Fluids Engineering Conference (2019).



Sangjin Ryu is an Associate Professor with the Department of Mechanical and Materials Engineering, the University of Nebraska-Lincoln (UNL), Lincoln, NE, USA, and a faculty member of Nebraska Center for Materials and Nanoscience, Lincoln, NE, USA. Dr. Ryu received the B.S. and M.S. degrees in Mechanical Engineering from Seoul National University, Seoul, South Korea, in 1997 and 1999, respectively, and the Ph.D. degree in Mechanical Engineering from Massachusetts Institute

of Technology, Cambridge, ME, USA, in 2009. Dr. Ryu worked as a researcher for Daewoo Commercial Vehicle, Gunsan, Korea, during 1999–2001 and Agency for Defense Development, Daejeon, Korea, during 2001–2004. He also worked as a postdoctoral researcher at Brown University, Providence, RI, USA, during 2009–2011. Dr. Ryu was the recipient of the Graduate Study Abroad Scholarship from Korea Science and Engineering Foundation (2004–2006), UNL College Distinguished Teaching Award and Holling Family Master Teacher Award from UNL (2019), and Outstanding Faculty Award from UNL Pi Tau Sigma (2019). Dr. Ryu's research interests include microfluidics, interfacial fluid dynamics and cell mechanics.